Nano-Analysis of DNA Conformation Changes Induced by Transcription Factor Complex Binding Using Plasmonic Nanodimers

Hiroyuki Morimura,[†] Shin-Ichi Tanaka,[‡] Hidekazu Ishitobi,[†,‡] Tomoyuki Mikami,[‡] Yusuke Kamachi,[‡] Hisato Kondoh,[‡] and Yasushi Inouye[†,‡,§,*]

[†]Department of Applied Physics, 2-1 Yamada-oka, Suita, Osaka 565-0871, Japan, [‡]Graduate School of Frontier Biosciences, 1-3 Yamada-oka, Suita, Osaka 565-0871, Japan, and [§]Photonics Advanced Research Center, Osaka University, 2-1 Yamada-oka, Suita, Osaka 565-0871, Japan

ABSTRACT The plasmon resonant wavelength for a pair of gold nanoparticles, or gold nanodimer, increases inversely with the gap distance between the two nanoparticles. Taking advantage of this property, we performed nanoscale measurements of DNA conformation changes induced by transcription factor binding. Gold nanoparticles were bridged by double-stranded DC5 DNA that included binding sequences for the transcription factors SOX2 and PAX6, which interact on the DC5 enhancer sequence and activate transcription. The gold nanodimers bound by SOX2 shifted the plasmon resonant wavelength from 586.8 to 604.1 nm, indicating that SOX2 binding induces DNA bending. When the SOX2 formed a ternary complex with PAX6 on DC5, the plasmon resonant wavelength showed a further shift to 611.6 nm, indicating additional bending in the DC5 sequence. Furthermore, we investigated DNA conformation changes induced by SOX2 and PAX6 on the DC5-con sequence, which is a consensus sequence of DC5 for the PAX6 binding region that strengthens the PAX6 binding but at the same time disrupts SOX2—PAX6-dependent transcriptional activation. When the PAX6 binding sequence in DC5 was altered to DC5-con, the plasmon resonant wavelength shifted much less to 606.5 nm, which is more comparable to the 603.9 nm by SOX2 alone. These results demonstrate that SOX2—PAX6 cobinding induces a large conformation change in DC5 DNA.

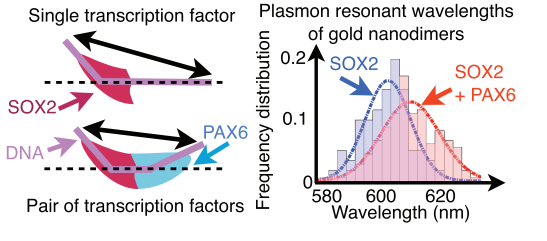

KEYWORDS: local surface plasmon · nanodimer · DNA conformation change · transcription · SOX2 · PAX6

The local surface plasmon is a resonant phenomenon of free electrons that collectively oscillate in noble metal nanoparticles (hereafter referred to as "NP") and the electric field of incident light.[1−5] Since metal NPs scatter incident light strongly at the plasmon resonant wavelength, metallic NPs have been widely used as biomolecular tags in single-molecular tracking studies.[6] As the proximity of two metallic NPs shortens, the frequency of the collective oscillation decreases because of the electrostatic attraction due to the surface charge, and the plasmon resonant wavelength lengthens.[7,8] Therefore, the gap distance between two NPs can be determined at less the diffraction limit by measuring the plasmon resonant wavelengths. Already, this strategy has been used to detect short DNA-associated events such as DNA double-strand hybridization[9−11] and the enzymatic cleavage of DNA.[12,13] In this paper, we applied the plasmon resonance for pairs of gold NPs (hereafter referred to as "gold nanodimers") to study a more elaborate process: DNA conformation changes induced by the binding of transcription factor complexes. In practice, nanodimers are formed by bridging two gold NPs using double-stranded DNAs that have binding sequences for the transcription factor complexes. Here, DNA conformation changes induced by the binding of a single transcription factor or transcription factor complex were measured as shifts in the plasmon resonant wavelength, which indicated shortening in the gap distance as the DNA bends.

The transcription factor SOX2 (SRY-related-HMG-box 2) and other SOX proteins

* Address correspondence to ya-inouye@ap.eng.osaka-u.ac.jp.

Received for review July 16, 2013 and accepted November 6, 2013.

Published online November 06, 2013
10.1021/nn403625s

play major roles in the regulation of developmental processes from early embryogenesis to various tissue stem cells by binding to target DNA sequences related to CATTGTT.[14,15] Two important features are involved in the functional interaction of SOX proteins with the target DNA. First, as SOX2 protein interacts with DNA at the minor groove, the minor groove widens and the DNA bends. Crystallography and NMR-based measurements of SOX−target DNA complexes have indicated that DNA can bend up to 90° by SOX binding depending on the target DNA sequence.[16−19]

The second and more important of the two features is that the binding of SOX protein alone to DNA does not elicit any gene activation, whereas the binding of SOX−partner transcription factor heterodimers does. Because the partner factor also requires a binding sequence, the functional SOX2 binding site is defined as the SOX−partner complex binding sequence.[14,15,20] Classic examples of SOX2−partner complexes are the SOX2−POU5f1 (OCT3/4) heterodimer, which regulates ES and iPS cells,[21,22] and the SOX2−PAX6 heterodimer, which regulates development of the visual system.[20,23]

The best-studied example of interactions between SOX2−partner complexes and DNA sequences is the binding of the SOX2−PAX6 complex to the 35 bp DC5 enhancer of the delta-Crystallin gene. The binding sequence for PAX6 as a complex in the DC5 sequence deviates from the consensus sequence for the binding of PAX6 alone[24] and is bound poorly by PAX6 in the absence of SOX2. The actual DC5 sequence is AAT ATT **CAT TGT T**GT TG*C TCA CCT ACC ATG GAT C*C, where SOX2 and PAX6 binding regions are bold and italic underlined, respectively. However, when complexed, PAX6 and SOX2 cooperatively and strongly bind to their respective DC5 binding sites and strongly activate the adjoining reporter gene, a reaction called transactivation.[20] For example, when the PAX6 binding sequence of the DC5 enhancer is replaced with the PAX6 binding consensus (DC5-con: AAT ATT **CAT TGT T**Ga TG*t TCA Cgc AtC ATG GAT C*C, where lower-case letters indicate base changes to match the PAX6 binding consensus sequence), the cooperation in binding between PAX6 and SOX2 is diminished, and the complex fails to activate the reporter gene.[20]

Circumstantial evidence suggests that when SOX2 and PAX6 together bind to the native sequence of DC5, the two protein factors interact strongly to form a tight complex, whereas interaction of the same two factors bound to the DC5-con sequence is less tight, resulting in differences in the complex formation on the bound DNA and the transactivation potential.[17,20] However, direct experimental evidence for this model is lacking.

We therefore adopted the plasmon resonance analysis using gold nanodimers to investigate the model. The rationale for our approach is that conformation changes of DNA will be larger in the case of a tight SOX2−PAX6 complex than that of SOX2 alone, and differences in the complex formation when using DC5 and DC5-con DNAs will be distinguished by the degree of the DNA conformation changes. The plasmon resonant wavelength was used to compare DNA conformations with DC5 and DC5-con sequences that were bound by SOX2 alone or SOX2 and PAX6 together, with the results strongly supporting the aforementioned model. As it is common that transactivation by SOX−partner factor complexes depends on the partner factor binding sequence,[14,15] this study demonstrates the importance of the ternary interaction among SOX factors, partner factors, and their binding to target DNA for gene activation.

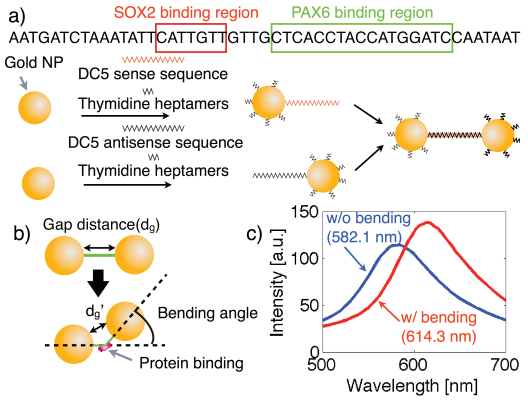

Figure 1. (a) Schematic of the gold nanodimer synthesis. (b) Model of a gold nanodimer before and after DNA bending induced by SOX2. (c) Calculated scattering spectrum of a gold nanodimer of 50 nm diameter and DNA bridge of 50 bp without (blue) and with bending (red).

RESULTS

Optimal Experimental Conditions for Gold Nanodimers Using the Finite Differential Time Domain Method. Gold nanodimers bridged by the DC5 sequence were prepared as follows. Two gold nanoparticles were each attached to a sense or antisense DC5 sequence *via* a thiol group and excess thymidine heptamers. Annealing the complementary DC5 strands formed the gold nanodimer, while coating of the particles with thymidine heptamers prevented gold nanoparticle aggregation (Figure 1a).

Noting that the binding of a transcription factor(s) induces DNA bending and shortening in the gap distance, we determined optimum parameters for detecting such changes, that is, the diameter of the gold NP and the length of the DNA bridge. Assuming a bending angle of 65°, which is based on a previous estimate from the circular permutation assay,[25] we calculated plasmon resonant wavelength shifts using the finite differential time domain (FDTD) method (Figure 1b). We did not consider using gold NPs with diameters above 60 nm, as otherwise the full width at half-maximum (fwhm) of the scattering spectrum becomes too broad due to a retardation effect and multipolar contribution,[26] which hinders accurate determination of the plasmon resonant peak, even

TABLE 1. Plasmon Resonant Peak Shifts and Ratios of Peak Shift Change to Gap Distance Change Assuming a Bending Angle of 65° upon SOX2 Binding (ϕ, NP Diameter; $\Delta\lambda$, Peak Wavelength Shift; Δd_g, Gap Distance Change)

ϕ (nm)	bp	$\Delta\lambda$ (nm)	Δd_g (nm)	$\Delta\lambda/\Delta d$
30	70	5.9	8.7	0.7
	60	7.5	8.2	0.9
	50	9.3	7.6	1.2
	40	16.5	7.1	2.3
40	70	8.5	10.3	0.8
	60	11.7	9.7	1.2
	50	17.9	9.2	1.9
	40	32.4	8.7	3.7
50	70	15.5	11.8	1.3
	60	22.9	11.3	2.0
	50	32.2	10.8	3.0
60	70	27.1	13.4	2.0
	60	35.0	12.9	2.7

though larger NPs generate stronger scattered light.[27] Hence, we investigated gold NPs with diameters between 30 and 60 nm. As for DNA length, we examined those between 40 to 70 base pairs (bp) because double-stranded DNAs shorter than 75 bp behave as rigid rods.[28] As shown in Table 1, we obtained values of the peak shift ($\Delta\lambda$) relative to the gap distance shortening (Δd). Among the conditions considered for maximizing $\Delta\lambda/\Delta d$ value, we excluded that where two gold NPs collide upon DNA bending caused by the cobinding SOX2 and PAX6 (namely, 40 nm diameter, 40 bp length) (Supporting Information Figure S1). Thus, a combination of NPs with 50 nm diameter and DNA with 50 bp length was selected. Using this condition, we calculated the scattering spectra of gold nanodimers for wavelengths ranging between 500 and 700 nm (Figure 1c). The scattering peak appears at 582.1 nm without DNA bending but shifts 32.2 to 614.3 nm when assuming 65° bending in the middle of the DNA.

Experimental Calibration of Gap-Distance-Dependent Plasmon Resonant Wavelengths. To calibrate the plasmon resonant wavelength of the gap distance, we synthesized 50 nm gold nanodimers using varied DNA lengths (15, 20, 25, and 50 bp) and measured the corresponding plasmon resonant wavelengths experimentally, rather than relying on FDTD-based numerical models, because the latter includes too many assumptions. The gap distance was defined as the sum of the DNA length (0.34 nm per bp) and short-chain hexane (C6) thiol linker (0.9 nm)[29] at both ends of the DNA. We measured the scattering spectrum of individual gold nanodimers using a spectrometer equipped with an electron multiplying CCD camera. In total, 26 specimens were measured for nanodimers bridged by DNA of 15, 20, or 25 bp and 64 nanodimers bridged by 50 bp. A typical scattering spectrum is shown in Figure S2. Before each spectrum was acquired, a polarizer was

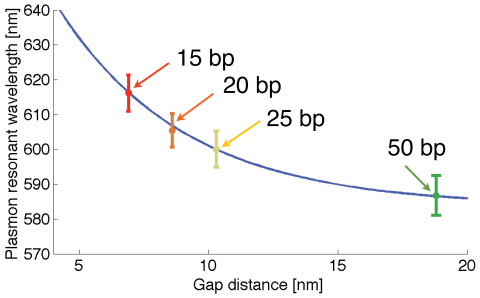

Figure 2. Mean plasmon resonant wavelengths of gold nanodimers of different interparticle distances (15, 20, 25, and 50 bp). Error bars show standard deviations. The blue line shows an exponential fit of the mean wavelengths.

rotated to set the polarization to the nanodimer axis in order to distinguish the gold nanodimer from an unpaired monomer or higher order aggregates. The frequency distributions of the plasmon resonant wavelengths of the measured spectra are shown in Figure S3. The mean and standard deviations were determined by fitting a cumulative Gaussian function to each cumulative frequency distribution. The mean plasmon resonant wavelengths were 616.2 ± 5.2, 606.5 ± 4.8, 600.1 ± 5.2, and 586.8 ± 5.7 nm when using DNA bridges of 15, 20, 25, and 50 bp length, respectively, showing an exponential decay (Figure 2).[30]

Conformation Change of DC5 DNA upon Binding of SOX2 and the SOX2–PAX6 Complex. A suspension of 50 nm diameter gold nanodimers each bridged by DNA of 50 bp and containing the DC5 sequence was divided into four aliquots that were mixed with nothing, PAX6, SOX2, or SOX2 plus PAX6 protein preparations, respectively. Scattering spectra were measured from 64 nanodimers for the first three specimens and from 196 nanodimers for the fourth. Averaged and normalized scattering spectra of gold nanodimers in the presence of no transcription factor, SOX2, and SOX2 + PAX6 are shown in Figure S4. Figure 3 and Table 2 summarize the frequency distribution of the plasmon resonant wavelengths using the wild-type DC5 sequence. Mean wavelengths were determined by fitting a cumulative Gaussian function to each cumulative frequency distribution. In the aliquot absent of transcription factors, which represents unbent DNA, the mean plasmon resonant peak was 586.8 ± 5.7 nm (Figure 3a, peak A1). The addition of PAX6 did not alter the peak position (587.7 ± 7.5 nm, Figure 3b, peak A2), whereas the addition of SOX2 shifted the plasmon peak to 604.1 ± 7.7 nm and caused an estimated bending angle of 61.3° in the middle of the SOX2 binding region (Figure 3c, peak A3). The addition of SOX2 and PAX6 together shifted the plasmon peak even further to 611.6 ± 9.8 nm (Figure 3d, peak A4). These results indicate that binding of the SOX2–PAX6 complex causes a larger conformation change to the DC5

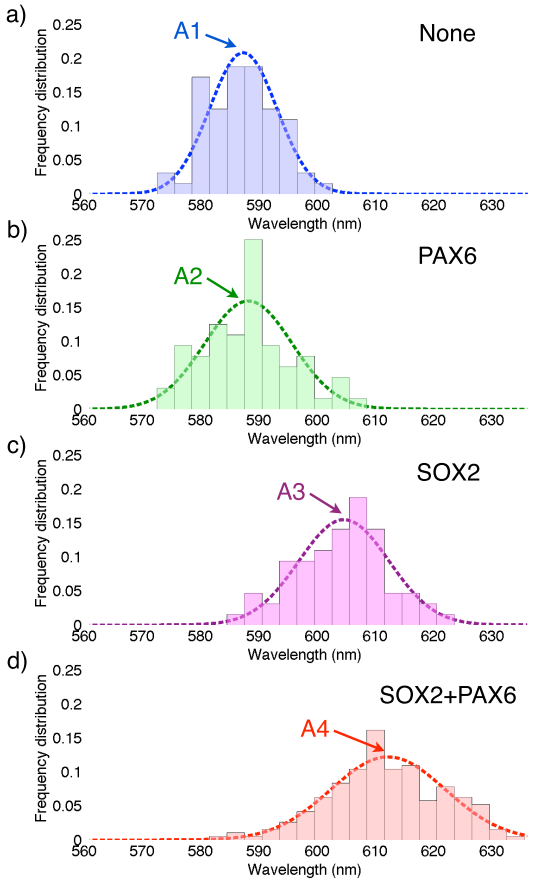

Figure 3. Frequency distributions of the plasmon resonant wavelengths of gold nanodimers with DNA bridges that had a length of 50 bp and included the DC5 sequence in the presence of (a) no transcription factor, (b) SOX2, (c) PAX6, and (d) both SOX2 and PAX6. A1 to A4 shows each peak positions.

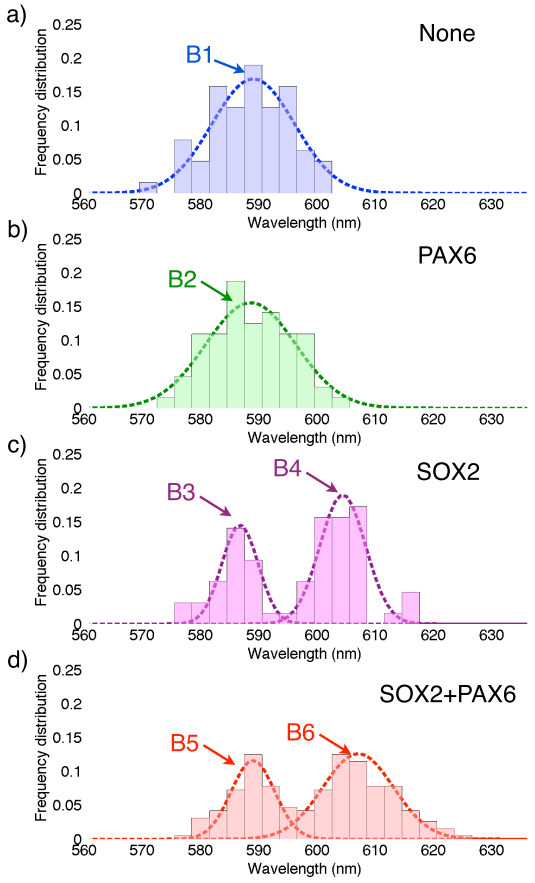

Figure 4. Frequency distributions of the plasmon resonant wavelengths of gold nanodimers with DNA bridges that had a length of 50 bp and included the DC5-con sequence in the presence of (a) no transcription factor, (b) SOX2, (c) PAX6, and (d) both SOX2 and PAX6. B1 to B6 shows each peak positions.

TABLE 2. Plasmon Resonant Peaks and Interparticle Distances of Gold Nanodimers[a]

transcription factor	plasmon peak (nm)	gap distance (nm)	DNA end distance (nm)
DC5 + none (A1)	586.8 ± 5.7	18.8	18.8
DC5 + PAX6 (A2)	587.7 ± 7.5		
DC5 + SOX2 (A3)	604.1 ± 7.7	9.2	16.3
DC5 + SOX2 + PAX6 (A4)	611.6 ± 9.8	7.7	16.1
DC5-con + none (B1)	588.5 ± 7.1		
DC5-con + PAX6 (B2)	588.1 ± 7.7		
DC5-con + SOX2 (B4)	603.9 ± 3.9	9.3	16.3
DC5-con + SOX2 + PAX6 (B6)	606.5 ± 6.1	8.7	16.2

[a] A1—A4 and B1—B6 indicate the peak positions in Figures 3 and 4, respectively.

sequence than that by SOX2 alone and brings the two ends of the DC5 sequence significantly closer.

The same set of experiments were done using the DC5-con sequence, which binds to PAX6 more strongly than DC5 but also lacks enhancer activity (Figure 4, Table 2). In the absence of a transcription factor, the peak of the frequency distribution of the plasmon resonant wavelengths was 588.5 ± 7.1 nm (Figure 4a, peak B1). This value is similar to that observed for the DC5 sequence. The addition of PAX6 had no effect on this value (588.1 ± 7.7 nm, Figure 4b, peak B2). Upon the addition of SOX2, however, two peaks at 586.2 ± 3.1 nm (Figure 4c, peak B3) and 603.9 ± 3.9 nm (Figure 4c, peak B4) were detected. The former value was not statistically different from the peak seen in the absence of transcription factors (B1) according to Welch's *t* test ($\alpha = 0.01$). This fact and the ratio of the peaks suggest that 40% of the gold nanodimers were not bound by SOX2, and the remaining 60% fraction of the SOX2-bound DC5-con DNA was bent in the same fashion as the DC5 wild-type sequence (Figure 3c, peak A3). This result is consistent with our earlier observation that SOX2 binds DC5-con less efficiently.[20] Finally, the addition of SOX2 together with PAX6 changed the frequency distribution of the plasmon resonant wavelengths; the peak of the SOX2-unbound fraction was 588.5 ± 3.7 nm (Figure 4d, peak B5), which mimics B1, while the second peak position shifted to 606.5 ± 6.1 nm (Figure 4d, peak B6), which is a much weaker effect than that when using the DC5 sequence (611.6 ± 9.8 nm, Figure 3d, peak A4).

The above results indicate a large conformation change of DC5 DNA upon the binding of SOX2 and PAX6 that cannot be explained by simple additive effects from the single bindings of SOX2 or PAX6. This large conformation change of DNA was not detected when using DC5-con, even though the sequence is bound by both SOX2 and PAX6. Thus, our observations are the first to demonstrate experimentally that the functional binding of the SOX2−PAX6 complex requires a specific DNA sequence for the PAX6 binding site like that found in DC5, and that its binding induces a large conformation change in the DNA.

DISCUSSION

Parameters That May Affect Plasmon Resonant Wavelength. We measured the plasmon resonant wavelength of gold nanodimers to estimate the gap distance and DNA conformation changes induced by the binding of transcription factors. To evaluate the reliability of this measurement, we considered other parameters that may affect the plasmon resonant wavelength. For instance, we observed variations of several nanometers in the mean plasmon resonant wavelength of gold nanodimers with DNA bridges of the same length; the mean wavelength of nanodimers with the DC5 sequence was 586.8 nm, while that with the DC5-con sequence was 588.5 nm. One factor we explored was the surface coverage of the gold NPs by short (3.3 nm) single-stranded DNAs (thymidine heptamers), which were used to prevent nanoparticle aggregation. We assumed that the refractive index (RI) of the 3.3 nm dielectric layer formed by single-stranded DNA is proportional to the surface coverage by the DNA (for example, 0% surface coverage = RI of 1.337, 50% = 1.400, and 100% = 1.462). The plasmon resonant wavelength of the gold nanodimer changed 0.06 nm per 1% change in the surface coverage according to numerical analysis using the FDTD method. Thus, a 30% difference in surface coverage results in a 2 nm plasmon resonant wavelength difference. Such variations in the surface coverage could result from the sample preparation. The diameter of the gold nanoparticles was also a factor we investigated, as it varied ±4% in the preparations. We analyzed the plasmon resonant wavelength of gold nanodimers of diameters 48, 50, and 52 nm using the FDTD method, finding plasmon resonant wavelengths of 579.1, 582.1, and 584.9 nm, respectively. Hence, variations in the diameter could also influence the plasmon resonant wavelength. Finally, we examined the potential effects of placing proteins between the gold nanoparticles because proteins have a high refractive index (~1.6).[31] We performed FDTD calculations upon inserting two dielectric rods between the gold nanoparticles, one having a RI of double-stranded DNAs (RI = 1.53, length = 18.8 nm, diameter = 2 nm)[32] and the other having a RI of proteins (RI = 1.6, length = 10 nm, diameter = 2 nm).

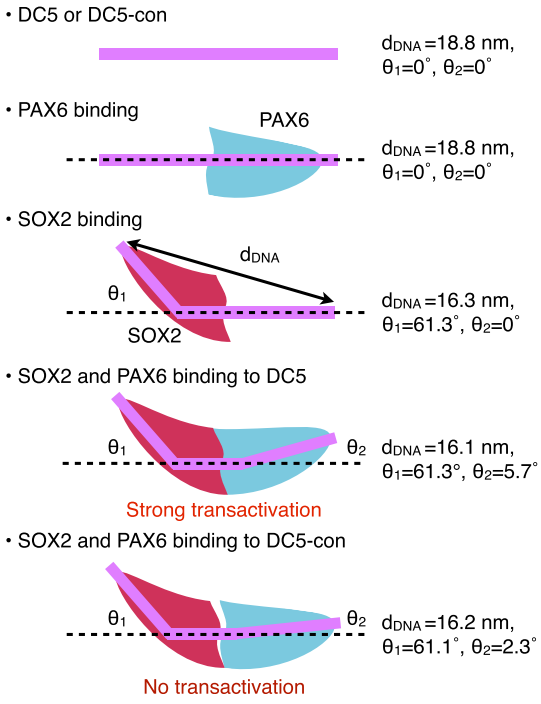

Figure 5. Model of DNA conformation changes induced by SOX2 and PAX6. The purple bar illustrates DNA; red and cyan represent the transcription factors SOX2 and PAX6, respectively; d_{DNA}, θ_1, and θ_2 refer to the DNA end distance, bending angle at the SOX2 sites, and that at the PAX6 sites, respectively.

The calculated plasmon resonant wavelengths were 582.4 nm with double-stranded DNA and protein and 582.1 nm with double-stranded DNA only. We thus concluded that the plasmon resonant wavelength is not significantly affected by the binding of proteins to the DNA bridge.

Conformation Change of DC5 DNA upon Binding of SOX2 and the SOX2−PAX6 Complex. Despite the effects of the above factors, changes in the plasmon resonant wavelength of DC5 DNA-bridged nanoparticles were such that they unequivocally demonstrate a large conformation change in the DNA. From the gap distances indicated by the plasmon resonant wavelengths, we estimated the distances between the termini of DNA 50 bp (18.8 nm) long (Figure 5). Upon the binding of SOX2 to the SOX2 site, the gap distance shortened to 9.2 nm, which corresponds to a bending angle of 61.3° when assuming simple bending in the middle of the SOX2 site. Binding of the SOX2−PAX6 complex caused the gap distance to shorten even more to 7.7 nm, suggesting that an additional conformation change was supposedly induced in the PAX6-interacting region of the DNA. Because the DC5 sequence is presumably bent at a minimum of two sites by the binding of the SOX2−PAX6 complex, the second bending angle in the PAX6 binding region was estimated to be 5.7° (Figure 5). In the present experiments, the protein domains of SOX2 (1−202 from the 315 aa full-length SOX2) and PAX6 (1−169 from the 422 aa full-length

PAX6) used in the experiments included the DNA binding domain and relatively short C-terminal extensions. The results indicate that these protein moieties are sufficient for establishing a strong interaction between SOX2 and PAX6. This observation is consistent with our earlier biochemical assay using EMSA, which found the same protein moieties bind cooperatively to the DC5 DNA sequence.[20] Using the DC5-con sequence, however, cobinding of SOX2 and PAX6 induced only slightly greater bending in the DNA than did SOX2 alone and resulted in a gap distance of 8.7 nm, which corresponds to only 2.3° bending in the PAX6-interacting DNA region (Figure 5). The DC5-con sequence, further, is known to show no enhancer (transactivation) activity despite the cobinding.[20] Thus, our DNA conformation analysis demonstrates that the cobinding of SOX2 and PAX6 to DNA is not sufficient for transcriptional activation, which instead requires a tight interaction between the two protein factors upon binding to the wild-type DC5 sequence (Figure 5).

Comparison of Plasmon Resonant Wavelength Analysis with FRET-Dependent Measurements of DNA Conformation Changes. The plasmon resonant wavelength shift provides a very powerful tool for the analysis of DNA conformation changes. Because the polarization exerted on a gold nanodimer is always parallel to the incident light, the plasmon resonant wavelength is determined by the gap distance and the polarization of the incident light. Additionally, only the scattered light from the nanodimers is required. This scattered light is brighter than that emitted by single chromophores and also means that our method suffers from neither photoblinking nor photobleaching. Förster resonance energy transfer (FRET) is often used to measure distances between biological molecules of interest. However, FRET is limited to DNA distances of a few to 10 nm due to the small amplitude of electronic transition dipoles, whereas the plasmon resonant wavelength can measure gap distances that range several to 20 nm. Another method, nanometal surface energy transfer (NSET), was reported to measure a wider range of distances than FRET but does not alleviate the problem of photoblinking or photobleaching.[33] In a recent report, DNA duplexes were prepared such that they had the fluorescent donor and acceptor molecules located at two respective termini, three artificial kinks caused by unpaired adenine residues and an inserted binding sequence for bacterial catabolite activator protein (CAP).[34] The distance between the DNA termini was 7.2 nm on average (average FRET efficiency, 0.29) without CAP binding but increased to 8.8 nm (average FRET efficiency, 0.11) when bound by CAP. The data therefore distinguished the CAP-bound and unbound states of the DNA owing to the conformation changes caused by CAP binding. However, the accuracy of the local DNA conformation changes is difficult to assess by this method because of fluctuations in the hinge angles.

Comparison with Circular Permutation Assay. A different biochemical approach, the circular permutation assay, uses acrylamide gel electrophoresis and can estimate the angle of DNA bending upon the binding of transcription factors like SOX.[35] When a bend is induced in a DNA of a few hundreds base pairs, the DNA electrophoresis is retarded with the bend's sharpness and its location to the center of the DNA. We have estimated the bending in DC5 induced by SOX2 to be 66°.[25] Further, this assay is excellent at comparing the effects of different proteins on DNA bending when using the same experimental condition. However, the estimation of bending angles is based on various assumptions, meaning the circular permutation assay can only provide a very rough estimate of the macroscopic bending angle in a long DNA and not the nanoscale information obtained from plasmon resonant wavelength analysis.

CONCLUSIONS

Our plasmon resonant wavelength analysis method, which is based on the optical properties of gold NPs, has various advantages for measuring DNA conformation changes. In this study, we applied this method to measuring the conformation changes induced by SOX2–PAX6 binding of DNA that bridged two gold NPs. Taking the plasmon resonant wavelengths after the addition of one or two transcription factors, we constructed a nanoscale model of the conformation change of DC5 DNA, finding two bends. This conformation change is a consequence of a strong SOX2–PAX6–DNA ternary complex, which is required for potent transcription activation. The present study considered only the equilibrium state of transcription factor binding to DNA. Real-time measurements of DNA cleavage by EcoRV using gold nanodimers suggest that our method has the potential for measuring DNA conformation changes in real time, as well.[13]

METHODS

FDTD Numerical Analysis. We used the FDTD method to analyze the plasmon resonant wavelength of gold nanodimers (Fullwave 6.2, R-Soft). The spatial domain had three dimensions in Cartesian coordinates (Figure S5), and the grid size was 1 nm. The center of a gold nanodimer was set at the origin, (0,0,0), and the nanodimer axis corresponded to the *y*-axis. The range of the spatial domain was −135 nm to +135 nm in the *x*–*y* plane and −150 nm to a sum of 250 nm plus a quarter of the wavelength in the *z*-axis. This spatial domain was enclosed by perfectly matching layers and divided into two different refractive index regions separated by the dashed line. One had a RI = 1.337, which corresponds to phosphate buffered saline (PBS), and the other a RI = 1.500, which corresponds to the coverslip. Gold NPs were covered with a dielectric layer of single-stranded DNA and RI = 1.462 and irradiated by a monochromatic incident light.

The scattered electric field (E-field) was acquired in a curved region of 130 × 130 nm^2 in the $x-y$ plane. This region covered the E-field obtained by an objective lens with NA = 0.8. The sum of the squared E-field in all grids of this region was set to the scattered light intensity. The scattering spectrum was acquired by changing the wavelength of incident light. The plasmon resonant wavelength was determined by fitting the Lorentzian function to the spectrum.

Preparation of Gold Nanodimers. Gold nanoparticles were purchased from BBInternational. Double-stranded DNAs to bridge the gold nanoparticles were purchased from Life Technologies and had the following sequences (sense, antisense): 50 bp DC5 sequence, 5′-AAT GAT CTA AAT ATT CAT TGT TGT TGC TCA CCT ACC ATG GAT CCA ATA AT and 5′-ATT ATT GGA TCC ATG GTA GGT GAG CAA CAA CAA TGA ATA TTT AGA TCA TT; 50 bp DC5-con sequence, 5′-AAT GAT CTA AAT ATT CAT TGT TGA TGT TCA CGC ATC ATG GAT CCA ATA AT and 5′-ATT ATT GGA TCC ATG ATG CGT GAA CAT CAA CAA TGA ATA TTT AGA TCA TT; 25 bp DNA bridge, 5′-AAT GAT CTA AAT ATT CAT TGT TGT T and 5′-AAC AAC AAT GAA TAT TTA GAT CAT T; 20 bp DNA bridge, 5′-TCT AAA TAT TCA TTG TTG TT and 5′-AAC AAC AAT GAA TAT TTA GA; and 15 bp DNA bridge, 5′-ATA TTC ATT GTT GTT and 5′-AAC AAC AAT GAA TAT. All DNA sequences had a short-chain hexane (C6) thiol at the 5′-terminal. Three DNA solutions were initially prepared: 1 μM sense strand target DNA, 1 μM antisense target DNA, and 60 μM thymidine heptamer in 10 mM borate buffer, pH 7.4. Because thiol groups at the terminal of DNA sequences easily form disulfide bonds, the disulfide bonds in the DNAs were cleaved by dithiothreitol (DTT) (125 mM for thymidine heptamers and 10 mM for target DNA) at room temperature for 30 min. DTT was removed by filtration through a NAP-5 column (GE Healthcare). Then the thymidine heptamers were mixed with sense or antisense target DNA to give a molar ratio of 50:1 and lyophilized at −80 °C for 2 h. The lyophilized DNAs were mixed with a suspension of gold nanoparticles and incubated at 50 °C for 24 h. The molar ratio of gold NP/target DNA/thymidine heptamer was 1:160:8000 for target DNAs of length 50 bp and 1:320:8000 for shorter DNAs (25, 20, and 15bp). NaCl (0.1 M) and phosphate buffer (pH 7.0) were added to the suspension, and the final concentration of Na ions was 0.1 M. The mixture was then incubated at room temperature for 48 h and centrifuged at 14 000 rpm for 30 min twice to remove unbound DNAs. Suspensions containing the sense or antisense target DNA were mixed at the same DNA concentration and incubated at 50 °C for 24 h for hybridization. Transcription factors SOX2 and PAX6 in 4-(2-hydroxyethyl)-1-piperazine ethane sulfonic (HEPES) buffer solution (55 mM KCl, 22 mM HEPES-NaOH (pH 7.9) and 0.2 mM *N*-ethylmaleimide) were added to a suspension of gold nanodimers bridged by DC5 or DC5-con DNA at a molar ratio of transcription factor to gold nanodimers of 100:1 and incubated for 30 min for their binding. A coverslip (ϕ 25 mm, Fischer Scientific) was sonicated in ethanol and then immersed in 1.0 vol % 3-aminopropyltrimethoxysilane (APTMS, Shin-Etsu Chemical) for 4 min. After the coverslip was functionalized by the silane, a solution of gold nanodimers with or without transcription factors (SOX2 and/or PAX6) was incubated on the coverslip for 5 min, and the solution with unbound gold nanodimers was blown away. The coverslip was immediately placed in a sample holder that was then filled with phosphate buffered saline (pH 7.4, Na^+ 153 mM, K^+ 4 mM), the ionic strength of which does not affect DNA lengths.[10,27] Gold nanodimers used for plasmon wavelength measurements typically constituted 20% of the final preparation according to scanning electron microscopy (Figure S6) and were distinguished from monomers (no polarization) and higher aggregation (brighter scattering) by dark-field microscopy.

Binding of SOX2/PAX6 to DC5 DNA Sequences. DNA binding domains for the SOX2 and PAX6 moiety were expressed in insect cells and bacterial cells, respectively, and purified, as described previously.[20] The DNA binding activities of the transcription factor preparations were confirmed by electrophoretic mobility assay.

Microscopy. A dark-field optical microscope (Eclipse Ti, Nikon) equipped with a 100 W halogen lamp, dark-field condenser (oil immersion type, NA = 1.2−1.43), and an oil immersion objective lens (100×, NA = 0.8) was used. Images were magnified by 1.5× through a relay lens. Scattered light from individual gold nanodimers was acquired by a spectrometer equipped with an electron multiplying CCD camera (SR303, Andor) or a cooled digital camera (DS-U2 Nikon). The slit size was 100 μm, and the line density of the grating was 600 lines/mm. The resolution of the spectrometer was approximately 1 nm, and the wavelength accuracy was ±0.2 nm. One spectrum was taken in 1 s and accumulated 10 times. Finally, the acquired spectra were fitted to a Lorentzian function.

Conflict of Interest: The authors declare no competing financial interest.

Acknowledgment. We thank Dr. Peter Karagiannis for reading the manuscript. This work was supported by Grants-in-Aid for Scientific Research 25118513 (Innovative areas "Transcription Cycles") to Y.I. and 22247035, 23657007, and 25113713 to H.K. from the Ministry of Education, Culture, Sports, Science and Technology, Japan.

Supporting Information Available: Supplementary figures This material is available free of charge *via* the Internet at http://pubs.acs.org.

REFERENCES AND NOTES

1. Ichimura, T.; Hayazawa, N.; Hashimoto, M.; Inouye, Y.; Kawata, S. Tip-Enhanced Coherent Anti-Stokes Raman Scattering for Vibrational Nanoimaging. *Phys. Rev. Lett.* **2004**, *92*, 220801.
2. Ichimura, T.; Watanabe, H.; Morita, Y.; Verma, P.; Kawata, S.; Inouye, Y. Temporal Fluctuation of Tip-Enhanced Raman Spectra of Adenine Molecules. *J. Phys. Chem. C* **2007**, *111*, 9460–9464.
3. Kawata, S.; Inouye, Y.; Verma, P. Plasmonics for Near-Field Nano-Imaging and Superlensing. *Nat. Photonics* **2009**, *3*, 388–394.
4. Tanaka, Y.; Kaneda, S.; Sasaki, K. Nanostructured Potential of Optical Trapping Using a Plasmonic Nanoblock Pair. *Nano Lett.* **2013**, *13*, 2146–2150.
5. Kühn, S.; Håkanson, U.; Rogobete, L.; Sandoghdar, V. Enhancement of Single-Molecule Fluorescence Using a Gold Nanoparticle as an Optical Nanoantenna. *Phys. Rev. Lett.* **2006**, *97*, 017402.
6. Nan, X.; Sims, A. P.; Xie, X. S. Organelle Tracking in a Living Cell with Microsecond Time Resolution and Nanometer Spatial Precision. *ChemPhysChem* **2008**, *9*, 707–712.
7. Nordlander, P.; Oubre, C.; Prodan, E.; Li, K.; Stockman, M. I. Plasmon Hybridization in Nanoparticle Dimers. *Nano Lett.* **2004**, *4*, 899–903.
8. Grillet, N.; Manchon, D.; Bertorelle, F.; Bonnet, C.; Broyer, M.; Cottancin, E.; Lermé, J.; Hillenkamp, M.; Pellarin, M. Plasmon Coupling in Silver Nanocube Dimers: Resonance Splitting Induced by Edge Rounding. *ACS Nano* **2011**, *5*, 9450–9462.
9. Sönnichsen, C.; Reinhard, B. M.; Liphardt, J.; Alivisatos, A. P. A Molecular Ruler Based on Plasmon Coupling of Single Gold and Silver Nanoparticles. *Nat. Biotechnol.* **2005**, *23*, 741–745.
10. Chen, J. I. L.; Chen, Y.; Ginger, D. S. Plasmonic Nanoparticle Dimers for Optical Sensing of DNA in Complex Media. *J. Am. Chem. Soc.* **2010**, *132*, 9600–9601.
11. Verdoold, R.; Gill, R.; Ungureanu, F.; Molenaar, R.; Kooyman, R. P. H. Biosensors and Bioelectronics Femtomolar DNA Detection by Parallel Colorimetric Darkfield Microscopy of Functionalized Gold Nanoparticles. *Biosens. Bioelectron.* **2011**, *27*, 77–81.
12. Liu, G. L.; Yin, Y.; Kunchakarra, S.; Mukherjee, B.; Gerion, D.; Jett, S. D.; Bear, D. G.; Gray, J. W.; Alivisatos, A. P.; Lee, L. P.; *et al.* A Nanoplasmonic Molecular Ruler for Measuring Nuclease Activity and DNA Footprinting. *Nat. Nanotechnol.* **2006**, *1*, 47–52.
13. Reinhard, B. M.; Sheikholeslami, S.; Mastroianni, A.; Alivisatos, A. P.; Liphardt, J. Use of Plasmon Coupling To Reveal the Dynamics of DNA Bending and Cleavage by Single EcoRV

Restriction Enzymes. *Proc. Natl. Acad. Sci. U.S.A.* **2007**, *104*, 2667–2672.
14. Kamachi, Y.; Uchikawa, M.; Kondoh, H. Pairing SOX Off: With Partners in the Regulation of Embryonic Development. *Trends Genet.* **2000**, *16*, 182–187.
15. Kondoh, H.; Kamachi, Y. SOX-Partner Code for Cell Specification: Regulatory Target Selection and Underlying Molecular Mechanisms. *Int. J. Biochem. Cell Biol.* **2010**, *42*, 391–399.
16. Werner, M. H.; Huth, J. R.; Gronenborn, A. M.; Clore, G. M. Molecular Basis of Human 46X,Y Sex Reversal Revealed from the Three-Dimensional Solution Structure of the Human SRY-DNA Complex. *Cell* **1995**, *81*, 705–714.
17. Reményi, A.; Lins, K.; Nissen, L. J.; Reinbold, R.; Schöler, H. R.; Wilmanns, M. Crystal Structure of a POU/HMG/DNA Ternary Complex Suggests Differential Assembly of Oct4 and SOX2 on Two Enhancers. *Genes Dev.* **2003**, *17*, 2048–2059.
18. Palasingam, P.; Jauch, R.; Ng, C. K. L.; Kolatkar, P. R. The Structure of SOX17 Bound to DNA Reveals a Conserved Bending Topology but Selective Protein Interaction Platforms. *J. Mol. Biol.* **2009**, *388*, 619–630.
19. Scaffidi, P.; Bianchi, M. Spatially Precise DNA Bending Is an Essential Activity of the SOX2 Transcription Factor. *J. Biol. Chem.* **2001**, *276*, 47296–47302.
20. Kamachi, Y.; Uchikawa, M.; Tanouchi, A.; Sekido, R.; Kondoh, H. PAX6 and SOX2 Form a Co-DNA-Binding Partner Complex That Regulates Initiation of Lens Development. *Genes Dev.* **2001**, *15*, 1272–1286.
21. Yuan, H.; Corbi, N.; Basilico, C.; Dailey, L. Developmental-Specific Activity of the FGF-4 Enhancer Requires the Synergistic Action of SOX2 and Oct-3. *Genes Dev.* **1995**, *9*, 2635–2645.
22. Takahashi, K.; Yamanaka, S. Induction of Pluripotent Stem Cells from Mouse Embryonic and Adult Fibroblast Cultures by Defined Factors. *Cell* **2006**, *126*, 663–676.
23. Inoue, M.; Kamachi, Y.; Matsunami, H.; Imada, K.; Uchikawa, M.; Kondoh, H. PAX6 and SOX2-Dependent Regulation of the SOX2 Enhancer N-3 Involved in Embryonic Visual System Development. *Genes Cells* **2007**, *12*, 1049–1061.
24. Epstein, J. A.; Glaser, T.; Cai, J.; Jepeal, L.; Walton, D. S.; Maas, R. L. Two Independent and Interactive DNA-Binding Subdomains of the PAX6 Paired Domain Are Regulated by Alternative Splicing. *Genes Dev.* **1994**, *8*, 2022–2034.
25. Kamachi, Y.; Cheah, K. S.; Kondoh, H. Mechanism of Regulatory Target Selection by the SOX High-Mobility-Group Domain Proteins as Revealed by Comparison of SOX1/2/3 and SOX9. *Mol. Cell. Biol.* **1999**, *19*, 107–120.
26. Kelly, K. L.; Coronado, E.; Zhao, L. L.; Schatz, G. C. The Optical Properties of Metal Nanoparticles: The Influence of Size, Shape, and Dielectric Environment. *J. Phys. Chem. B* **2003**, *107*, 668–677.
27. Busson, M. P.; Rolly, B.; Stout, B.; Bonod, N.; Larquet, E.; Polman, A.; Bidault, S. Optical and Topological Characterization of Gold Nanoparticle Dimers Linked by a Single DNA Double Strand. *Nano Lett.* **2011**, *11*, 5060–5065.
28. Williams, L. D.; Maher, L. J. Electrostatic Mechanisms of DNA Deformation. *Annu. Rev. Biophys. Biomol. Struct.* **2000**, *29*, 497–521.
29. Hill, R. T.; Mock, J. J.; Hucknall, A.; Wolter, S. D.; Jokerst, N. M.; Smith, D. R.; Chilkoti, A. Plasmon Ruler with Angstrom Length Resolution. *ACS Nano* **2012**, *6*, 9237–9246.
30. Jain, P. K.; Huang, W.; El-Sayed, M. A. On the Universal Scaling Behavior of the Distance Decay of Plasmon Coupling in Metal Nanoparticle Pairs: A Plasmon Ruler Equation. *Nano Lett.* **2007**, *7*, 2080–2088.
31. Jung, L. S.; Campbell, C. T.; Chinowsky, T. M.; Mar, M. N.; Yee, S. S. Quantitative Interpretation of the Response of Surface Plasmon Resonance Sensors to Adsorbed Films. *Langmuir* **1998**, *14*, 5636–5648.
32. Elhadj, S.; Singh, G.; Saraf, R. F. Optical Properties of an Immobilized DNA Monolayer from 255 to 700 nm. *Langmuir* **2004**, *20*, 5539–5543.
33. Yun, C. S.; Javier, A.; Jennings, T.; Fisher, M.; Hira, S.; Peterson, S.; Hopkins, B.; Reich, N. O.; Strouse, G. F. Nanometal Surface Energy Transfer in Optical Rulers, Breaking the FRET Barrier. *J. Am. Chem. Soc.* **2005**, *127*, 3115–3119.
34. Crawford, R.; Kelly, D. J.; Kapanidis, A. N. A Protein Biosensor That Relies on Bending of Single DNA Molecules. *ChemPhysChem* **2012**, *13*, 918–922.
35. Ferrari, S.; Harley, V. SRY, Like HMG1, Recognizes Sharp Angles in DNA. *EMBO J.* **1992**, *1*, 4497–4506.